JOM Journal of Optical Microsystems

RESEARCH PAPER

Overcoming challenges in fabrication of beam shaping meta-optics using sensitive mr-EBL resist

Jerin Geogy George* **and Shanti Bhattacharya**
Indian Institute of Technology Madras, Department of Electrical Engineering, Applied Optics Group, Chennai, Tamil Nadu, India

ABSTRACT. Shaping light to meet the needs of diverse optical applications is of utmost importance. Beam shaping allows one to alter the properties of light, enabling more complex behavior not possible with standard beams, such as Gaussian beams. Such beams have been generated using diffractive optics and more recently, meta-optics. For the latter, standard fabrication processes using electron beam lithography with the popular polymethyl methacrylate resist exist. However, there are several challenges due to the sub-wavelength features. We propose an alternate fabrication approach using a highly sensitive resist called mr-EBL resist. We show how the use of this resist reduces the patterning time, as well as the number of process steps. The process is explained with a case study on the fabrication of a meta-optical element that generates a modified Bessel beam with special properties.

 [DOI: 10.1117/1.JOM.4.4.041402]

Keywords: meta-optics; nanophotonics; mr-EBL resist; Bessel beam

Paper 23043SS received Dec. 31, 2023; revised Apr. 11, 2024; accepted May 18, 2024; published Sep. 27, 2024.

1 Introduction

Optical beam shaping is of significant interest in diverse fields; including microscopy, material processing, and communication. This is because beam-shaping can enhance the properties of light making it more useful for many applications.[1] The generation of structured light with unique properties has been explored extensively. Examples include Bessel[2] and Airy[3] beams, known for their non-diffracting and self-healing ability, Laguerre Gaussian beams[4] possessing phase singularities, Mathieu beams[5] with invariant optical fields, etc. While various parameters of the light can be manipulated to generate shaped light, phase manipulation is one of the most efficient ways to do so. The phase-manipulating element can be as simple as a refractive or diffractive lens. However, more complex behavior also requires more complex structures, such as arrays of nanostructures capable of arbitrary phase modulation. Certain tailor-made designs may require a spatially random phase variation and may not be efficient or easy to realize using refractive optics or simple diffractive optics. Multi-level diffractive optics could impart random phase variations with reasonable efficiency.[6] They are, however, difficult to fabricate due to the requirement of multiple lithography steps. Spatial light modulators are also popular devices that have greater control for imparting arbitrary phase variations.[7] These devices are especially useful when tunability is required or for testing out ideas during the design and development process. However, they do not have the resolution of fabricated devices. In addition, their size would increase the overall dimensions of the optical instrument they are incorporated into, which might not align with the design goals or practicality of the intended system.

*Address all correspondence to Jerin Geogy George, ee20d029@smail.iitm.ac.in

Metasurfaces have over the last decade emerged as an efficient and relatively simpler way of creating phase elements, particularly those of an arbitrary nature.[8] Fabrication of meta-lenses with high efficiency,[9] achromatic behavior,[10] and polarization insensitivity,[11] etc., has been demonstrated by many researchers. Given the nanometer-scale dimensions inherent to metasurfaces, the electron beam (e-beam) lithography process has become the predominant choice for fabrication. Despite being a well-established fabrication method, e-beam lithography suffers from a low fabrication throughput. For mass production of meta-optical elements, deep UV or nanoimprint lithography may be more viable.[8,12] Table 1 presents a comparison of the popular lithography techniques utilized in the fabrication of meta-optics.

Typically, meta-optical elements fabricated with e-beam lithography struggle with size scalability due to lengthy patterning times and high computational demands for complex pattern processing.[15,24,25] This puts a constraint on using the element for a real application or even simply testing it.[26] Some of the parameters that determine the patterning time are the sensitivity of the e-beam resist as well as the patterning current of the e-beam system.[24] The popular positive e-beam resist, poly methyl methacrylate (PMMA) has a relatively low sensitivity necessitating higher exposure doses (200 to 400 $\mu C/cm^2$ at 30 keV) for effective patterning. Furthermore, PMMA has low etch resistance and is not typically used as a mask for etching.[27] Negative resists, such as hydrogen silsesquioxane (HSQ) and maN-2400, offer high-resolution patterns suitable for meta-optics. While HSQ possesses good etch selectivity, it requires a very high exposure dose (above 1000 $\mu C/cm^2$) and removal with hydrofluoric acid, which is not compatible with quartz substrates.[28] maN-2400 has better sensitivity than PMMA but exhibits moderate etch selectivity to silicon.[29] The utilization of ultra-sensitive mr-EBL resist has been demonstrated for high-throughput patterning of diffraction gratings and has good dry etch selectivity for etching silicon.[30] Our group has recently employed mr-EBL resist for patterning a meta-optical aberration correction element.[31] In this paper, we present for the first time the fabrication process flow of meta-optics using mr-EBL resist for realizing polysilicon nanostructures. To provide additional context to our approach, Table 2 compares the key strengths and limitations of popular e-beam resists, including mr-EBL, highlighting their suitability for patterning meta-optics.

In the fabrication of meta-optical elements typically composed of quartz/glass substrates, a charging effect during e-beam patterning is encountered.[36] Employing a high e-beam current can reduce patterning time, but it may lead to heating and charging effects in substrates where conductivity is not good.[24,37] The use of highly sensitive mr-EBL resist can effectively reduce the patterning time even when employing a low beam current.[30] Another critical consideration is the ease of pattern transfer from the resist to the material responsible for phase variation.

Table 1 Comparison of common lithography techniques used in meta-optics fabrication.

Method	Advantages	Disadvantages	Refs.
Photolithography	• High throughput for mass production • Deep UV can give high-resolution	• Not flexible for rapid prototyping • Requires mask typically written by e-beam lithography	13–15
E-beam lithography	• Very high resolution (sub-10 nm) and precise control • Suitable for rapid prototyping and research development	• Low throughput (limits the size of the element) • Costly equipment and requires high maintenance	16, 17
Nanoimprint lithography	• Very high feature resolution (sub-10 nm) • High throughput and large-area patterning	• Master mold required (relies on e-beam lithography) • Demolding issues and pattern defects	18–21
Two-photon polymerization	• High resolution (down to 100 nm) and flexibility • Clean room facility not required	• Low throughput (layer-by-layer construction) • Expensive equipment and material compatibility issues	22, 23

Table 2 Different popular e-beam resists and comparison of their performance parameters.

Resist (tone)	Benefits	Drawbacks	Refs.
PMMA (positive)	• High resolution (sub-10 nm) • Good balance of sensitivity and contrast	• Low etch resistance • Risk of pattern collapse	27, 32
HSQ (negative)	• High resolution (sub-5 nm) • High dry etch resistance (can be used as hard mask)	• Limited shelf life • Relatively low sensitivity • Not suitable for glass substrates	28, 32
ZEP-520 (positive)	• High resolution (sub-20 nm) • High sensitivity • Good etch resistance	• Relatively expensive • Complex development and removal process	32, 33
maN-2400 (negative)	• High resolution (about 20 nm) • Sensitivity better than PMMA	• Sensitive to precise conditions of pre- and post-exposure bakes • Adhesion issues	29, 34
mr-EBL 6000 (negative)	• High sensitivity • High etch resistance • Good resolution (about 75 nm)	• Limited process data available • Sensitivity to process conditions	30, 35

The mr-EBL resist can also be employed as an etch mask for pattern transfer, ensuring a lower number of process steps compared to PMMA-based pattern transfer.[35,38]

To demonstrate the advantages of mr-EBL, we take the fabrication of a specific meta-optical element as a case study. In this paper, we focus on the fabrication of an element that produces a modified Bessel beam with reduced sidelobes. The final meta-optical element, which consists of polysilicon nanostructures, operates at 1064 nm. The element is fabricated by patterning using a 30 keV e-beam system (Raith 150 TWO) on the highly sensitive mr-EBL 6000.3 resist (Micro Resist Technology). While several researchers have demonstrated the successful fabrication of meta-optical elements, very few have discussed the challenges in fabricating those elements.[16,39] In our paper, we also discuss the challenges associated with the conventional fabrication process of meta-optics involving the use of PMMA resist with metal lift-off and highlight the benefits of using the mr-EBL negative resist.

2 Fabrication of Meta-Optical Elements

The meta-optical element that we have chosen as a case study is one that we have designed and fabricated earlier[40] using a conventional PMMA-based technique. The element generates a modified Bessel beam with reduced sidelobes, which is relevant for light-sheet imaging applications.[41] The phase profile of the element is generated through the spatial multiplexing of two axicon phase functions, optimized to minimize sidelobes.[40] The optimized opening angles of the axicons are 0.53 deg and 0.94 deg, respectively. In certain propagation regions, the sidelobes of the two coaxially propagating Bessel beams produced by the element interfere destructively, resulting in the modified Bessel beam with reduced sidelobes. While a simple axicon has a smoothly varying phase, achievable through refractive or multi-level diffractive optics, our element has a non-uniformly varying phase. Meta-optics is particularly well-suited for realizing such phase functions, as the meta-atoms can locally impart the desired phase shifts with precision. A representative figure of a meta-optical element is shown in Fig. 1(a).

The meta-atoms are structured on polysilicon, which is a dielectric material with a high refractive index and low absorption coefficient at the design wavelength. The meta-atoms of choice are cylindrical nanopillars due to the polarization independence they offer. Initially, the meta-atom simulations are carried out using the finite element method with COMSOL Multiphysics. In the simulation, the height and the radius of the cylinders are swept over a range of values to determine the combination that gives full wavefront control (0 to 2π phase variation). Subsequently, a look-up table is generated, with a fixed height and varying radius [Fig. 1(b)], that provides the full phase variation and high-uniform transmittance.[43] This look-up map is then used to spatially arrange the meta-atoms based on the arbitrary phase function. While numerous

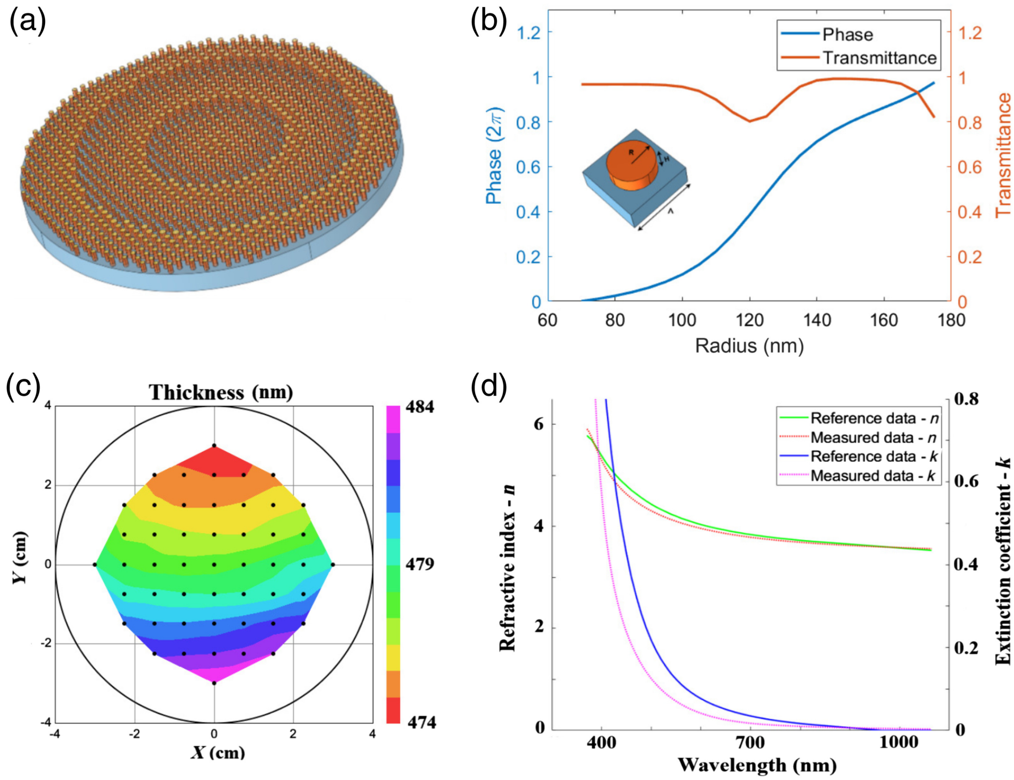

Fig. 1 (a) Sample illustration of a meta-optical element. (b) The phase and transmittance information of polysilicon cylindrical nanopillars with 480 nm pillar height. The wavelength used for simulation is 1064 nm. The period of the unit cell is 450 nm. (c) Thickness information at different points in a 4-in. wafer deposited with polysilicon using LPCVD at 640°C. (d) Optical constants of the deposited film compared against reference data.[42]

distinct meta-atoms can impart a significant number of phase levels, the fabrication tolerances impose limitations on the achievable number of phase levels. As per scalar diffraction theory, an eight-level realization of the arbitrary phase can achieve about 95% efficiency.[44] Following this, the desired phase is translated into an eight-level metasurface layout using the GDS package of Python software, facilitating the use of an e-beam system for patterning.

For preparing the sample before patterning, a quartz substrate is initially cleaned with acetone and isopropyl alcohol bath followed by oxygen plasma. Then, the substrate is coated with a 480 nm polysilicon film using a low-pressure chemical vapor deposition (LPCVD) technique at 640°C. Subsequently, the optical constants and thickness of the film are evaluated using a spectroscopic ellipsometer (M2000 - JA Woollam Co.). This step is done to ensure the validity of the meta-atom simulation for the deposited polysilicon film. Figures 1(c) and 1(d) show the data relating to the thickness and optical constants obtained from the ellipsometer measurement. It can be seen that the thickness of the film is nearly uniform throughout the substrate and the optical constants closely match the reference data.[42]

2.1 Challenges in Patterning Using e-Beam Lithography

After depositing the dielectric material, the subsequent step involves patterning, typically done using e-beam lithography given the sizes. Patterning resolution and time are critical considerations when using e-beam lithography. The instrument parameters must be optimized to efficiently achieve the smallest feature size necessary while maintaining reasonable patterning time. The choice of resist also contributes to the minimum feature size achievable. Depending on the specific patterning requirements, a positive or negative resist may be employed. In general, positive resists are used for patterning holes, while negative resists are preferred for patterning pillars.

2.1.1 *Patterning resolution*

A high acceleration voltage e-beam setting while patterning can result in better resolution with appropriate proximity correction. High-end e-beam systems, which are very expensive, have a maximum acceleration voltage of up to 100 keV while moderate systems have a maximum acceleration voltage of 30 keV. In a 100 keV system, the achievable resolution is about 1/10th the resist thickness while with a 30 keV system, it ranges from 1/2 to 1/3rd the resist thickness.[45,46] Although one can enhance patterning resolution by reducing resist thickness, this increases the challenges in the pattern transfer process.

For example, meta-optics fabrication with PMMA resist (positive-tone) typically follows a metallization and lift-off for making a hard mask for etching. In an ideal scenario, the lift-off process can be done with a PMMA thickness twice that of the metal film;[47] yet, practical applications may require resist thicknesses exceeding three times the metal thickness. Consequently, this imposes a constraint on the minimum thickness of the resist required for patterning, to achieve a required resolution with a specified acceleration voltage setting. With a higher acceleration voltage patterning, the thickness of the resist can be made higher, facilitating an easy lift-off. When using a negative resist, the etching can be done directly after patterning if the etch selectivity of the resist is good. In this case, the thickness of the resist determines the thickness of the underlying material that can be etched. Clearly, using a 100 keV system would be better for fabricating meta-optics, but these systems are expensive and require high exposure doses and hence, longer patterning times. Fabricating meta-optics with low acceleration voltage (below 30 keV) systems remains a challenge, necessitating careful considerations of trade-offs to attain satisfactory performance.

2.1.2 *Patterning time*

Conventional refractive and diffractive elements typically have a size in the order of centimeters. Due to time constraints associated with e-beam lithography patterning, researchers fabricate down-sized meta-optical elements to demonstrate the proof of concept. However, to use these meta-optical elements in a specific application (e.g., beam shaping), they need to be at least in the mm range. Even patterning millimeter-sized elements takes hours, especially when employing a low beam current in the pA range. The patterning time in an e-beam lithography patterning can be calculated from[24]

$$\text{Exposure time} = \frac{\text{Exposure dose} \times \text{Exposure area}}{\text{Electron beam current}}.$$

PMMA requires an exposure dose ranging from 200 to 400 $\mu\text{C/cm}^2$ when using a 30 keV acceleration voltage. On the other hand, mr-EBL resists, require only about 10 to 15 $\mu\text{C/cm}^2$ for the same acceleration voltage. This can reduce the patterning time to < 20 times what is required with PMMA. Another way to reduce the patterning time is to opt for a larger beam current with a higher aperture. However, this may lead to the charging and drifting while patterning, especially if the substrate has low conductivity. Therefore, it is preferable to use the smallest beam current possible when patterning on such substrates. Furthermore, a lower aperture will provide better patterning, owing to the larger depth of focus of the e-beam.[37]

In our fabrication process, a polysilicon-deposited sample is then coated with mr-EBL 6000.3 resist and is subsequently patterned using a Raith 150 Two e-beam lithography system. The resist is uniformly coated at a spin speed of 3000 rpm, resulting in a thickness of ≈300 nm. After this, the resist is prebaked at 90°C for 5 min. Patterning is carried out at an acceleration voltage of 30 keV and a beam current of 18 pA, utilizing a 7.5 μm aperture. The exposure dose applied is only 15 $\mu\text{C/cm}^2$, a significantly lower value compared to other conventional e-beam resists, contributing to a reduction in patterning time. After patterning, the resist is post-baked at 110°C for 5 min, followed by development using mr-Dev 600 for 50 s.

Figure 2 shows the patterns on the resist after development. In Fig. 2(b), the cylinders that are designed to have circular shapes with the same diameter, exhibit varying shapes. This is mainly attributed to the charging-induced pattern distortion. Furthermore, edge roughness is also observed in the patterns after development. The altered shape as well as the edge roughness will

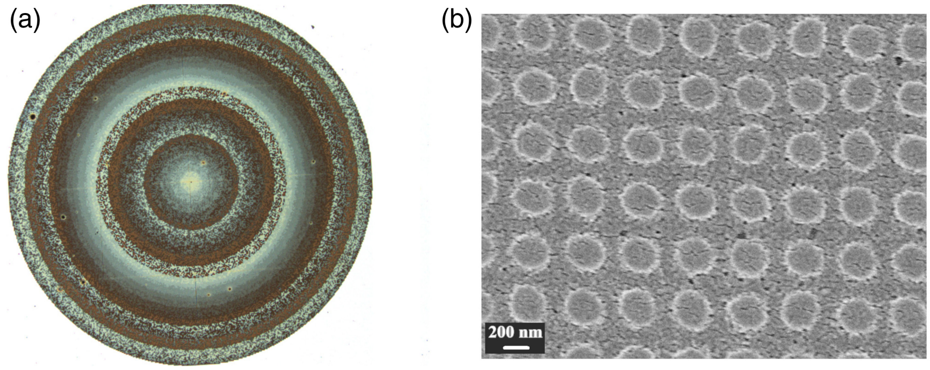

Fig. 2 Patterned resist after development. (a) Confocal microscope image of the pattern. (b) Scanning electron microscope (SEM) image of the resist pillars (imaged after gold coating).

result in distorted structures while etching. This will affect the diffraction efficiency of the meta-optical element.[37] By optimizing the dose factor and the development time, a good resist profile can be obtained.

2.2 Pattern Transferring: Challenges

When patterning using PMMA, a lift-off process commonly employing e-beam evaporation (due to its directionality) is used to create a metal mask for etching. By using the mr-EBL resist, the number of process steps before etching can be reduced. Furthermore, the lift-off process can be challenging in the case of nanostructures with a high aspect ratio (which is mostly the case in metasurfaces). One of the major disadvantages of using the lift-off-based approach involving e-beam evaporation is PMMA shrinkage and PMMA bubbling resulting in improper lift-off.[48] In certain instances, PMMA shrinkage may prevent successful lift-off and the application of ultrasonication can enhance lift-off. However, it comes with the potential risk of small, high aspect ratio structures collapsing. Figures 3(a) and 3(b) show such cases during PMMA lift-off.

The e-beam lithography patterning using mr-EBL resist can circumvent the challenges associated with the PMMA lift-off. After developing, the patterns on the mr-EBL resist are directly transferred to the underlying polysilicon by dry etching using inductively coupled plasma reactive ion etching. The etching process is done at a chamber pressure of 15 mTorr with SF_6 (5 sccm) and CHF_3 (18 sccm) etch gases. The radio frequency (RF) power used is 30 W and the ICP power used is 1000 W. Finally, the resist is removed by using oxygen plasma to complete the fabrication. The element fabricated has a diameter of 1 mm. It should also be noted that dry etching may not always result in anisotropic etching. Depending on the pressure as well as the RF and ICP power, the etching may result in an isotropic etch profile, as shown in Fig. 3(c).

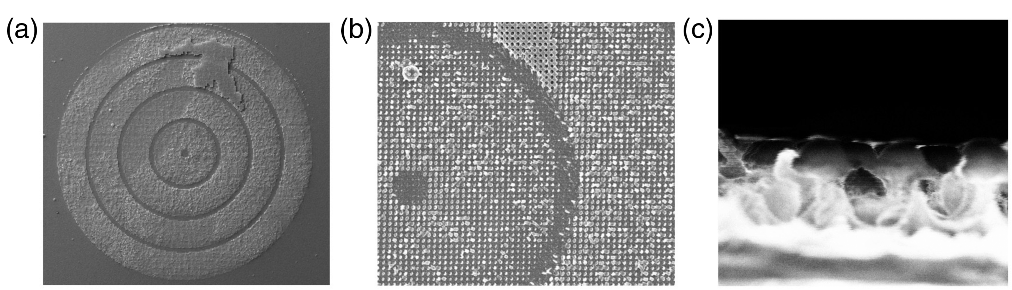

Fig. 3 (a) PMMA not properly lifted off. Lift-off is done after chromium deposition using e-beam evaporation. (b) Smaller structures were destroyed after PMMA lift-off using ultrasonication. (c) Isotropic etch profile after dry etching. SF6 etch (25 sccm) gas at 40 mTorr chamber pressure is used for etching. RF power used is 50 W and ICP power used is 0 W.

3 Optical Testing of the Meta-Optical Elements

We employed the process flow given in Fig. 4(a) to fabricate the meta-optical element. The fabricated element [Fig. 4(b)] successfully generates a modified Bessel beam with reduced sidelobes. The planar and the tilted images of the pillars are presented in Figs. 4(c) and 4(d), respectively. While cylindrical pillars exhibit imperfections, including distortion and surface roughness, they possess reasonably well-defined vertical sidewalls.

The meta-optical element was tested using a fiber-coupled laser source (MCLS1 - Thorlabs) at 1064 nm. A fiber collimator was employed to collimate the beam and the beam size was ensured to match the size of the meta-optical element. The modified Bessel beam has a periodic nature and exhibits reduced sidelobes in the vicinity of the propagation plane, where the longitudinal wavevectors of two co-propagating Bessel beams coincide ($z = 0$ plane). The period is calculated as $2\pi/|k_{z1} - k_{z2}|$,[49] resulting in a value of 47 mm for the fabricated element. This periodic behavior can be observed to the extent of the minimum depth of focus (61 mm) among the two Bessel beams. The modified Bessel beam is captured in the propagation region (centered about 47 mm) to observe the reduced sidelobes. Figure 5 shows the experimentally generated modified Bessel beam using the fabricated meta-optical element.

Analysis of Figs. 5(a) and 5(b) reveals that the modified Bessel beam exhibits a reduced sidelobe peak intensity. The standard Bessel beam has a sidelobe peak intensity of 16% that of the main lobe peak intensity. In contrast, the modified Bessel beam demonstrates a reduced sidelobe peak of 6.8% at the $z = 0$ plane. The $1/e^2$ radius of the generated beam is 51 μm, aligning closely with the design value of 44 μm. The sidelobe peak intensity of the generated beam remained below 10% over a propagation distance of about 20 mm. The two rings in the far field intensity profile [Fig. 5(c)] of the generated beam indicate two coaxially propagating Bessel beams. The far-field intensity profile also reveals the presence of a zeroth-order [inside the dotted circle in Fig. 5(c)]. This zeroth-order mainly arises due to the structural distortion which reduces the diffraction efficiency of the generated beam. The non-uniform nature of the phase function realized also plays a role in this unwanted zeroth order. The meta-atom simulation is done with a periodic boundary condition (assuming infinite periodicity) and any deviation from a periodic nature (which is the case practically) will result in phase variations. The zeroth-order beam can

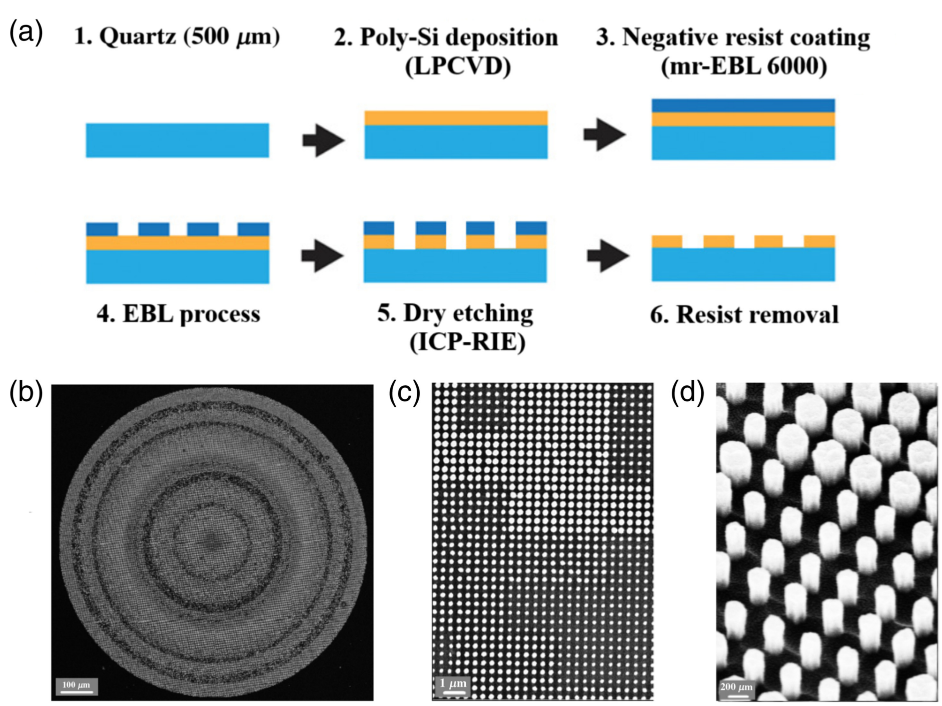

Fig. 4 Meta-optics fabrication. (a) Process flow of the fabrication with mr-EBL 6000.3 resist. SEM image of the (b) fabricated element, (c) planar view of the meta-atoms, and (d) tilted view of the meta-atoms.

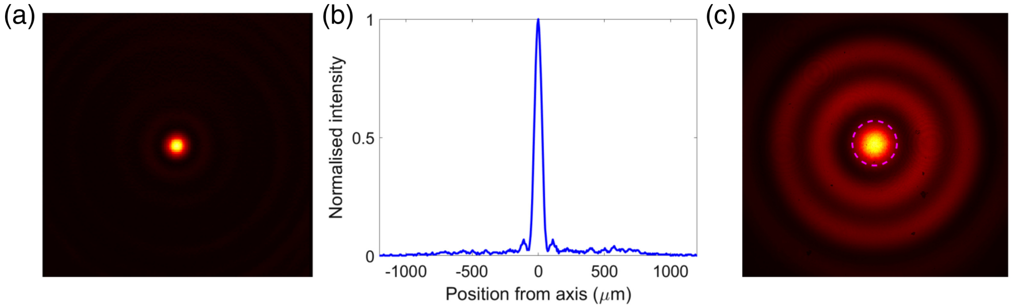

Fig. 5 Experimental results. (a) Cross-sectional intensity profile of the modified Bessel beam. (b) Line intensity profile along the x-axis of the modified Bessel beam. (c) Far-field intensity profile of the generated beam.

affect the propagation-invariant nature of the modified Bessel beam. With sophisticated design and fabrication, the presence of the zeroth order may be reduced, but it is a challenging task. Alternatively, spatial filtering in the Fourier space can remove the zeroth order, which is more practical.

4 Conclusions

We successfully fabricated a meta-element combining two axicon functions. This element efficiently generated a modified Bessel beam with reduced sidelobes. The fabrication of this meta-optical element was carried out using the relatively new highly sensitive negative resist, mr-EBL 6000.3. This choice enabled a significantly faster patterning process compared to conventional e-beam lithography employing the popular PMMA resist, particularly with low beam current. Our fabrication involves a minimal number of process steps, enhancing the throughput and reliability of meta-optics fabrication.

Code and Data Availability

Data underlying the results presented in this paper are not publicly available at this time but may be obtained from the authors upon reasonable request.

Acknowledgments

The authors acknowledge financial support from the Ministry of Human Resource Development, New Delhi through the SPARC project (SPARC/2018-2019/P796/SL). The fabrication for this work was done at the Centre for NEMS and Nanophotonics (CNNP) at IIT Madras funded by the Ministry of Electronics and Information Technology (MeitY) and the Department of Science and Technology (DST).

References

1. F. M. Dickey, *Laser Beam Shaping: Theory and Techniques*, CRC Press (2018).
2. J. Durnin, “Exact solutions for nondiffracting beams. I. The scalar theory,” *J. Opt. Soc. Am. A* **4**(4), 651–654 (1987).
3. G. Siviloglou et al., “Observation of accelerating airy beams,” *Phys. Rev. Lett.* **99**(21), 213901 (2007).
4. L. Allen et al., “Orbital angular momentum of light and the transformation of Laguerre-Gaussian laser modes,” *Phys. Rev. A* **45**(11), 8185 (1992).
5. J. C. Gutiérrez-Vega, M. Iturbe-Castillo, and S. Chávez-Cerda, “Alternative formulation for invariant optical fields: Mathieu beams,” *Opt. Lett.* **25**(20), 1493–1495 (2000).
6. S. Banerji et al., “Imaging with flat optics: metalenses or diffractive lenses?” *Optica* **6**(6), 805–810 (2019).
7. J. G. George, Y. Guruvaiah, and S. Bhattacharya, “Sidelobe-suppressed bessel beam using hologram,” in *Conf. Lasers and Electro-Opt./Pac. Rim*, Optica Publishing Group, p. P_CTu8_24 (2022).
8. N. Yu and F. Capasso, “Flat optics with designer metasurfaces,” *Nat. Mater.* **13**(2), 139–150 (2014).
9. Y. Wang et al., “High-efficiency broadband achromatic metalens for near-IR biological imaging window,” *Nat. Commun.* **12**(1), 5560 (2021).
10. S. Wang et al., “A broadband achromatic metalens in the visible,” *Nat. Nanotechnol.* **13**(3), 227–232 (2018).

11. M. Khorasaninejad et al., "Polarization-insensitive metalenses at visible wavelengths," *Nano Lett.* **16**(11), 7229–7234 (2016).
12. D. K. Oh et al., "Nanoimprint lithography for high-throughput fabrication of metasurfaces," *Front. Optoelectron.* **14**, 229–251 (2021).
13. L. Zhang et al., "High-efficiency, 80 mm aperture metalens telescope," *Nano Lett.* **23**(1), 51–57 (2022).
14. N. Li et al., "Large-area metasurface on CMOS-compatible fabrication platform: driving flat optics from lab to fab," *Nanophotonics* **9**(10), 3071–3087 (2020).
15. J.-S. Park et al., "All-glass, large metalens at visible wavelength using deep-ultraviolet projection lithography," *Nano Lett.* **19**(12), 8673–8682 (2019).
16. V.-C. Su et al., "Advances in optical metasurfaces: fabrication and applications," *Opt. Express* **26**(10), 13148–13182 (2018).
17. Y. S. Tan et al., "High-throughput fabrication of large-scale metasurfaces using electron-beam lithography with SU-8 gratings for multilevel security printing," *Photonics Res.* **11**(3), B103–B110 (2023).
18. A. M. Baracu et al., "Silicon metalens fabrication from electron beam to UV-nanoimprint lithography," *Nanomater* **11**(9), 2329 (2021).
19. C. A. Dirdal et al., "Towards high-throughput large-area metalens fabrication using UV-nanoimprint lithography and Bosch deep reactive ion etching," *Opt. Express* **28**(10), 15542–15561 (2020).
20. V. J. Einck et al., "Scalable nanoimprint lithography process for manufacturing visible metasurfaces composed of high aspect ratio TiO_2 meta-atoms," *ACS Photonics* **8**(8), 2400–2409 (2021).
21. M. D. Austin et al., "Fabrication of 5 nm linewidth and 14 nm pitch features by nanoimprint lithography," *Appl. Phys. Lett.* **84**(26), 5299–5301 (2004).
22. Z. Faraji Rad, P. D. Prewett, and G. J. Davies, "High-resolution two-photon polymerization: the most versatile technique for the fabrication of microneedle arrays," *Microsyst. Nanoeng.* **7**(1), 71 (2021).
23. K. Vanmol et al., "Fabrication of multilevel metalenses using multiphoton lithography: from design to evaluation," *Opt. Express* **32**(6), 10190–10203 (2024).
24. M. M. Greve and B. Holst, "Optimization of an electron beam lithography instrument for fast, large area writing at 10 kv acceleration voltage," *J. Vac. Sci. Technol. B* **31**(4), 043202 (2013).
25. A. She et al., "Large area metalenses: design, characterization, and mass manufacturing," *Opt. Express* **26**(2), 1573–1585 (2018).
26. H. Zheng et al., "Large-scale metasurfaces based on grayscale nanosphere lithography," *ACS Photonics* **8**(6), 1824–1831 (2021).
27. A. Grigorescu and C. Hagen, "Resists for sub-20-nm electron beam lithography with a focus on HSQ: state of the art," *Nanotechnology* **20**(29), 292001 (2009).
28. M. Rommel et al., "Sub-10 nm resolution after lift-off using HSQ/PMMA double layer resist," *Microelectron. Eng.* **110**, 123–125 (2013).
29. D. Andren et al., "Large-scale metasurfaces made by an exposed resist," *ACS Photonics* **7**(4), 885–892 (2020).
30. A. J. Taal, J. Rabinowitz, and K. L. Shepard, "mr-EBL: ultra-high sensitivity negative-tone electron beam resist for highly selective silicon etching and large-scale direct patterning of permanent structures," *Nanotechnology* **32**(24), 245302 (2021).
31. S. Thomas et al., "Metaoptics for aberration correction in microendoscopy," *Opt. Express* **32**(6), 9686–9698 (2024).
32. A. S. Gangnaik, Y. M. Georgiev, and J. D. Holmes, "New generation electron beam resists: a review," *Chem. Mat.* **29**(5), 1898–1917 (2017).
33. K. Koshelev et al., "Comparison between ZEP and PMMA resists for nanoscale electron beam lithography experimentally and by numerical modeling," *J. Vac. Sci. Technol. B* **29**(6), 06F306 (2011).
34. K. Kato et al., "Electron beam lithography with negative tone resist for highly integrated silicon quantum bits," *Nanotechnology* **32**(48), 485301 (2021).
35. C. Martin et al., "Electron beam lithography at 10 keV using an epoxy based high resolution negative resist," *Microelectron. Eng.* **84**(5–8), 1096–1099 (2007).
36. K. T. Arat et al., "Charge-induced pattern displacement in e-beam lithography," *J. Vac. Sci. Technol. B* **37**(5), 051603 (2019).
37. J. Zhang et al., "Charging effect reduction in electron beam lithography with nA beam current," *Microelectron. Eng.* **88**(8), 2196–2199 (2011).
38. A. J. Taal et al., "Toward implantable devices for angle-sensitive, lens-less, multifluorescent, single-photon lifetime imaging in the brain using Fabry–Perot and absorptive color filters," *Light Sci. Appl.* **11**(1), 24 (2022).
39. A. Patoux et al., "Challenges in nanofabrication for efficient optical metasurfaces," *Sci. Rep.* **11**(1), 5620 (2021).
40. J. G. George, K. Dholakia, and S. Bhattacharya, "Generation of bessel-like beams with reduced sidelobes for enhanced light-sheet microscopy," *Opt. Continuum* **2**(7), 1649–1660 (2023).

41. G. Di Domenico et al., "Cancellation of Bessel beam side lobes for high-contrast light sheet microscopy," *Sci. Rep.* **8**(1), 17178 (2018).
42. W. A. McGahan et al., "Optical characterization of polycrystalline silicon thin films," *Proc. SPIE* **2725**, 450–459 (1996).
43. R. Dharmavarapu et al., "Metaoptics: opensource software for designing metasurface optical element GDSII layouts," *Opt. Express* **28**(3), 3505–3516 (2020).
44. Z. Zhang et al., "Hybrid-level Fresnel zone plate for diffraction efficiency enhancement," *Opt. Express* **25**(26), 33676–33687 (2017).
45. M. Rooks et al., "Low stress development of poly (methylmethacrylate) for high aspect ratio structures," *J. Vac. Sci. Technol. B: Microelectron. Nanometer Struct. Process. Meas. Phenom.* **20**(6), 2937–2941 (2002).
46. J. Zhou and X. Yang, "Monte Carlo simulation of process parameters in electron beam lithography for thick resist patterning," *J. Vac. Sci. Technol. B: Microelectron. Nanometer Struct. Process. Meas. Phenom.* **24**(3), 1202–1209 (2006).
47. L. Shao et al., "Preparation and characteristic analysis of nanofacula array," *Sci. Rep.* **11**(1), 22140 (2021).
48. B. Sun et al., "Role of electron and ion irradiation in a reliable lift-off process with electron beam evaporation and a bilayer PMMA resist system," *J. Vac. Sci. Technol. B* **39**(5), 052601 (2021).
49. S. Chavez-Cerda et al., "Experimental observation of interfering Bessel beams," *Opt. Express* **3**(13), 524–529 (1998).

Jerin Geogy George is a PhD scholar at the Department of Electrical Engineering, IIT Madras. His primary research focuses on the design and generation of complex light using meta-optics. His research interests include the application of complex light for enhancing the performance of light-sheet and STED microscopy techniques.

Shanti Bhattacharya received her PhD in physics from the Indian Institute of Technology, Madras, in 1997. She was awarded the Alexander von Humboldt award in 1998 and worked at the Technical University of Darmstadt, Germany, for several years. She subsequently joined Analog Devices, Cambridge, USA, where she worked as a design engineer. She is currently a professor at the Department of Electrical Engineering, IIT Madras. She has served on the board of OSA (now called Optica) and is currently an associate editor of *Optical Engineering* and the *Journal of Optical Microsystems*. Her current research interests are meta and diffractive optics, optical MEMS, and studies relating to imaging techniques.